PCCP

Accepted Manuscript

This is an *Accepted Manuscript*, which has been through the Royal Society of Chemistry peer review process and has been accepted for publication.

Accepted Manuscripts are published online shortly after acceptance, before technical editing, formatting and proof reading. Using this free service, authors can make their results available to the community, in citable form, before we publish the edited article. We will replace this *Accepted Manuscript* with the edited and formatted *Advance Article* as soon as it is available.

You can find more information about *Accepted Manuscripts* in the Information for Authors.

Please note that technical editing may introduce minor changes to the text and/or graphics, which may alter content. The journal's standard Terms & Conditions and the Ethical guidelines still apply. In no event shall the Royal Society of Chemistry be held responsible for any errors or omissions in this *Accepted Manuscript* or any consequences arising from the use of any information it contains.

ROYAL SOCIETY OF CHEMISTRY

www.rsc.org/pccp

Mass partitioning effects in diffusion transport

Milos Kojic[1,2,3], Miljan Milosevic[2], Suhong Wu,[1] Elvin Blanco[1], Mauro Ferrari[1], Arturas Ziemys[1,*]

[1] - Houston Methodist Research Institute, Houston, TX 77030; [2] - Belgrade Metropolitan University - Bioengineering Research and Development Center BioIRC Kragujevac, 34000 Kragujevac, Serbia; [3] – Serbian Academy of Sciences and Arts,11000 Belgrade, Serbia.

* The corresponding author: 6670 Bertner Ave., R7-116, Houston, TX 77030. Tel: (713) 441 7320. Email: aziemys@houstonmethodist.org

Keywords: interface, diffusion, particle, drug release, logP

Abstract

Frequently mass exchange takes place in heterogeneous environment among several phases, where mass partitioning may occur at the interface of phases. Analytical and computational methods for diffusion do not usually incorporate molecule partitioning and masking the true picture of mass transport. Here we present a computational Finite Element methodology to calculate diffusion mass transport with partitioning phenomenon included and the analysis of the effects of partitioning. Our numerical results showed that partitioning controls equilibrated

Physical Chemistry Chemical Physics Accepted Manuscript

mass distribution as expected from analytics solutions. The experimental validation of mass release from drug-loaded nanoparticles showed that partitioning might even dominate in some cases with respect to diffusion itself. The analysis of diffusion kinetics in the parameter space of partitioning and diffusivity showed that partitioning is extremely important parameters in systems, where mass diffusivity is fast and that the concentration of nanoparticles can control payload retention inside nanoparticles. The computational and experimental results suggest that partitioning and physiochemical properties of phases play important, if not crucial, role in diffusion transport and should be included in studies of mass transport processes.

Introduction

Diffusion mass transport occurs in many physical processes for which the theoretical interpretation is well established. It was found that mass dissipates according to the Fickian theory. According to this theory, the mass flux *J* can be expressed as:

$$J = -D\frac{\partial c}{\partial x} \quad (1)$$

where *D* is the diffusion coefficient and *∂c/∂x* is the concentration gradient. This phenomenological relationship, known as the Fick law, is widely applied, from industry to medicine. Diffusion as a mass transport process is significantly present in bioengineering, especially in areas of drug delivery, where micro- and nanoparticles soaked with drugs are

Physical Chemistry Chemical Physics Accepted Manuscript

designed to release therapeutic payload with certain benefits over simple intravenous drug injection. The majority of drugs are hydrophobic substances, meaning that those chemical compounds prefer organic phase over water [1]. Analogous conditions could be found in chemical and other industries, where the transported mass has to change the solvent or it can be suspended. Then the question arises whether the affinity to certain phase affects the transport of molecules is such that the assumption that mas transport is driven by concentration gradient becomes invalid.

It is well known that partitioning phenomenon has a thermodynamic origin [2]. The partitioning coefficient *P* is defined phenomenologically as:

$$P = \frac{C_{oil}}{C_{water}} \qquad (2)$$

where C_{oil} is the concentration of molecules in oil, and C_{water} is the concentration in water, at the oil-water interface. In practice, partitioning of molecules is tested in octanol-1/water system and is expressed by a logarithm of *P*, *logP*. The logP is a common property of drug molecules used to characterize hydrophobicity of compounds. The influence of logP to drug transport was recognized in many experimental studies in which the mass release was governed by hydrophobicity; there, more hydrophobic compounds (higher logP) were released slower [3-8]. Consequently, in case drug release from nanoparticle, it can be found that the

Physical Chemistry Chemical Physics Accepted Manuscript

release process is more dependent on the partitioning of the drug, than on diffusion through the matrix of the nanoparticle [4].

Although there are numerous references on diffusion mass transfer from one phase to another, and developed methods to predict logP from chemical structure of a compound [9], the partitioning effect in transport is generally neglected. Frequently, mass diffusion is characterized by transport coefficient that is simply acquired by fitting D, *e.g.* in [10]. Several literature sources recognized the importance of partitioning in transport. For example, partitioning of surfactant was analytically analyzed in [11], where it was found that partitioning is important in the diffusion kinetics of mass equilibration for two-phase microfluidic flows. The best examples of the use of partitioning was found studying transdermal drug delivery [12-14] and stents [15].

Here we present a computational approach to include partitioning into the mass diffusion Finite Element (FE) model. Our FE models were initially developed according to the classical diffusion formulation [16, 17] and lately were modified to incorporate diffusivity changes at phase interface [18, 19]. In this study the mass partitioning is analyzed in a simplified system, then validated with experiments by using nanoparticles, and finally the interplay between partitioning and diffusion parameters was studied.

Methods

Physical Chemistry Chemical Physics Accepted Manuscript

MD simulations. The molecular dynamics simulations were carried out using NAMD 2.6 [20] with a TIP3P water model [21] and NVT ensembles. All molecules were simulated with the CHARMM22 force [22]. The system had dimension 6.5x6.5x13.5 nm (Figure 1A). Octanol slab was created of 6.5 nm thickness and solvated with water, in Periodic Boundary Conditions, and with approximately the same volume of water and oil phases. 24 molecules of *p*-ethyphenol (PEPH) were randomly placed through all volume of the system, so that 12 molecules would be located in water and 12 molecules – in octanol. The whole model was minimized, equilibrated and later production simulation executed for 20 ns using 2 fs integration step. Diffusion was analyzed by evaluating center-of-mass displacement of PEPH molecules and calculating diffusivity dependence on proximity to the fiber in a similar fashion like in [1]. PEPH molecule density distribution was calculated along z-axis and normalized.

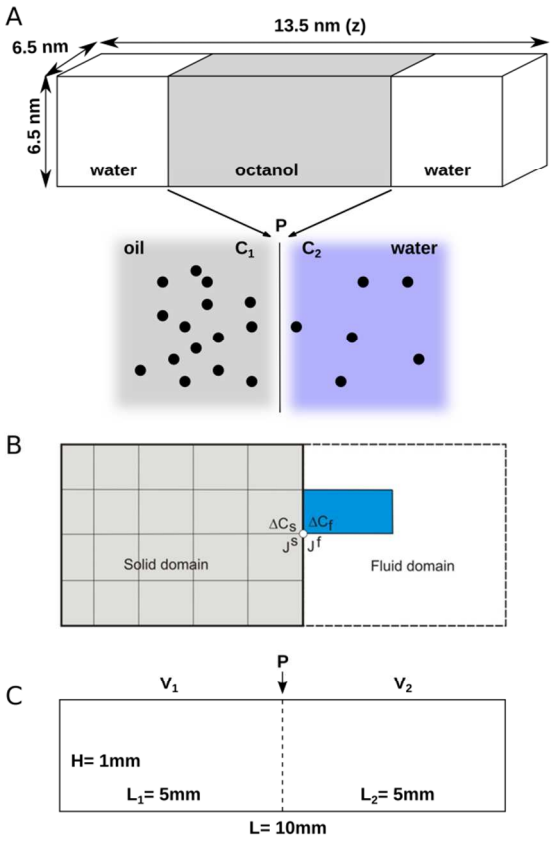

Physical Chemistry Chemical Physics Accepted Manuscript

Figure 1. Schematics of studied systems. (A) The structure and dimensions of MD model to simulate partitioning P between octanol and water phases. (B) Implementation of partitioning in the FE model, where increments of concentrations at the common node (J^S and J^f) are related as $\Delta C_f = p\Delta C_s$, equation (6).

FE simulations. A general form of FE balance equation for diffusion within an element can be written as [23]:

$$\left(\frac{1}{\Delta t}\mathbf{M}+\mathbf{K}\right)\Delta\mathbf{C} = \mathbf{Q}^{ext} - \left(\frac{1}{\Delta t}\mathbf{M}+\mathbf{K}\right)\mathbf{C} + \frac{1}{\Delta t}\mathbf{M}\mathbf{C}^t \quad (3)$$

where **M** and **K** are element matrices; C and C^t are nodal concentrations at the end and start of current time step of size Δt, and $\mathbf{Q}^{ext}$ is external flux.

The simplest way to express partitioning phenomena in molecular transport is to take that, within a time step, the ratio between number of molecules passing the boundary between two media (for easier representation we use solid-fluid boundary) is a constant *P*:

$$\Delta N_s / \Delta N_f = P \quad (4)$$

where ΔN_s and ΔN_f are the numbers at solid and fluid side, respectively. We will further use, for a convenience of implementation, a reverse value

$$p = 1/P \quad (5)$$

Physical Chemistry Chemical Physics Accepted Manuscript

Instead of the ratio of number of molecules we can relate increments of concentration (and concentrations) at the common point in solid and fluid, ΔC_s and ΔC_f, as

$$\Delta C_f = p\Delta C_s, \quad C_f = pC_s \tag{6}$$

Graphical illustration of the relations (6) is shown in Figure 1B. The relation (6) is further used to accordingly modify the matrices on the left side and nodal vectors on the right side of equation (3), for nodes at the interface between two media, before assembling equation (3) into the global system of balance for the entire diffusion domain, shown in Figure 1C and discussed further.

Validation experiments. The experiments pertaining to nanoparticles and payload release were published in [24]. The payload release data was used to validate computational transport analysis in this study. Further, only a brief description of experimental details is provided.

Nanoparticle fabrication: Rhodamine-containing nanoparticles comprised of poly(DL-lactide-co-glycolide) 50:50 (PLGA, inherent viscosity 0.95-1.20) were fabricated as described previously [24]. Briefly, a modified double emulsion procedure was employed, wherein rhodamine and polymer were dissolved in dichloromethane and added drop-wise to poly(vinyl alcohol) (PVA) under sonication. Following overnight evaporation, nanoparticles were collected and washed via centrifugation. The bodipy-containing cyclodextrin outer shell was prepared as described previously, involving overnight incubation of fluorophore and cyclodextrin. The final core-shell construct was assembled by incubating polymer nanoparticles and cyclodextrin as described previously.

Physical Chemistry Chemical Physics Accepted Manuscript

Release Study: Full details concerning fluorophore release, as in the case of nanoparticle fabrication and characterization can be found presented in [24]. Briefly, fluorophores were released into PBS and the concentration of both determined using a Synergy H4 Hybrid Reader and a previously established calibration curve. Release experiments were conducted in triplicate.

Results and Discussion

General MD model. The diffusion and partitioning phenomena are defined at molecular scale. We have simulated *p*-ethylphenol (PEPH) partitioning in octanol/water by using MD, as an academic example, before analyzing a more complex example with validation and studying deeper the effects of partitioning on diffusion transport. PEPH is a hydrophobic compound with logP = 2.5 which favors oil phase over water. At the initial time of MD simulation water and oil compartments accommodated the same number of PEPH (Figure S1A). During the initial 10 ns of MD simulation PEPH migrated from water phase to octanol phase, while PEPH in octanol remained in the same phase. Through the next 10 ns of MD simulation, PEPH molecules remained at equilibrium between both phases occupying mostly the octanol phase (Figure S1B). The calculated PEPH diffusivity across phases is shown in Figure S1C indicating that PEPH diffusivity in oil phase is 7 times lower ($0.2 \cdot 10^{-5}$ cm^2/s) than in water ($1.5 \cdot 10^{-5}$ cm^2/s). This simple model demonstrates that D describes transport efficiency in oil and water phases, while P gives the coupling between concentrations at the boundary of both phases.

Physical Chemistry Chemical Physics Accepted Manuscript

General FE model. By using the above described FE methodology, with incorporating mass portioning, we have formulated a macroscopic model (Figure 1C). The fully symmetrical model with the 1 x 10 mm dimensions was split into two equal compartments, with a virtual plane surface with partitioning. To demonstrate the effect of partitioning alone, the same diffusivity in both compartments was used. A 1 M concentration was prescribed at t = 0 for the left compartment and system was simulated up to 150 hours. Figure 2 shows the evolution of concentration profiles for logP = 0, 1, and 2. The comparison of the three systems shows that the higher concentration difference is achieved by increasing portioning, as expected analytically. In the system without partitioning (logP = 0) concentrations develop exponential profiles. But the systems with logP = 1 and 2 show increasingly evident partitioning of the mass. The calculated logP values for those systems are approximately 1.1 and 2.0 after 50 hours, which show an excellent match with the prescribed values in boundary conditions of the numerical continuum model.

Physical Chemistry Chemical Physics Accepted Manuscript

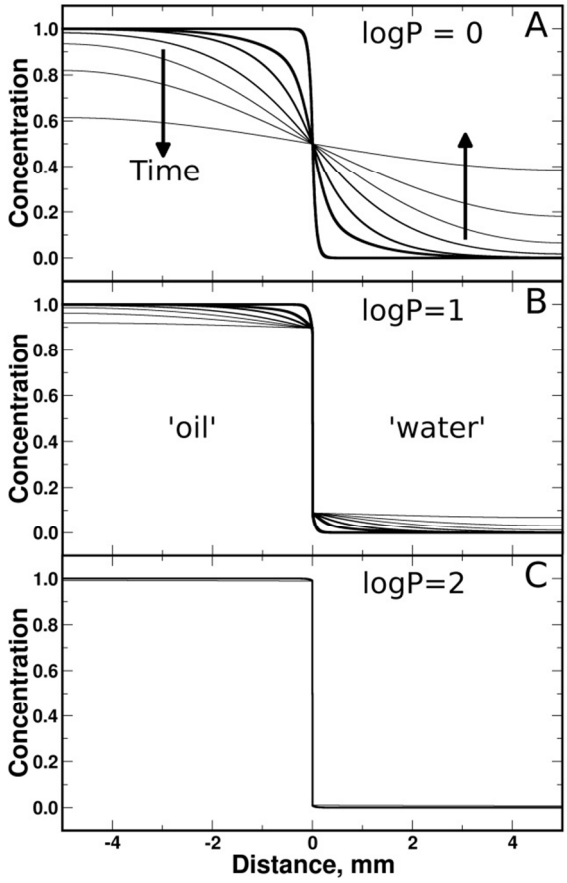

Figure 2. Mass redistribution in the fluidic system separated by imaginary phase separation plane surface at the zero coordinate. While diffusivities are equal on the left and right of the reservoir, those halves are separated by surface with different logP: (A) logP = 0 (no partitioning), (B) logP = 1, and (C) logP = 2.

Validation. We have applied our method to investigate the mass release from a polymeric particle that is a good example of potential applications, because there is a large amount of micro- and nanoparticles used in drug delivery. In general, most drugs are hydrophobic [25] and are loaded into polymeric or other particles. The representative diffusivity of molecules

Physical Chemistry Chemical Physics Accepted Manuscript

below 1 kDa of mass in water is in the order of 10^{-5} cm^2/s, while diffusivity within polymers are of the order of 10^{-8} cm^2/s [26]. Therefore, we can expect that other smaller molecules dissolved in polymers would diffuse by 10^3 orders slower than in water.

We have investigated the release of two molecules from the nested particle composed of core and thin shell (Figure 3A) as described and published previously in [24]. The PLGA core of the particle with radius of 52 nm was loaded with 0.167 M of Rhodamine B solution, while shell (18 nm thick) made of cyclodextrins was loaded with bodipy 630/650. The compounds have limited solubility in water with logP = 1.8 (Rhodamine B) and -0.3 (bodipy). Assuming the diffusivity of compounds could be reduced by polymer environment by 10^3 order, the characteristic diffusion length would be 0.1-1 μm, which exceeds the dimensions of the particle many times. Therefore, the payload release would happen in minutes, if not seconds. However, as the experiments showed in [24], the release from the shell was finalized within 40 hours and the release from the core was not finished within 100 hours; the data is re-plotted in Figure 3B. The best fit was calculated using logP = 10.3 and 11.3 for the shell and the core, correspondingly. Although different scaling factors were used to modify the payload diffusivity, the release was found to be controlled by partitioning only, as it was also noticed in [27]. That makes sense, because the size of particle is extremely small and the release exceeds substantially the theoretical limits attributable to a simple diffusive process.

Because of the partitioning effect, we also have a saturated release seen in Figure 3B, especially for Rhodamine B. Figure 3C displays the payload release from the core modeled with different logP values. It can clearly be seen that the increasing partitioning enables to account for the

Physical Chemistry Chemical Physics Accepted Manuscript

not released mass that is trapped inside the core of the particle. If no partitioning is used as in classical diffusion, the release would happen extremely fast. Therefore, taking into account the findings in this experimental example and in the general examples above, we can conclude that partitioning could be a fundamental phenomenon controlling mass exchange and can be even more important than diffusion transport.

Physical Chemistry Chemical Physics Accepted Manuscript

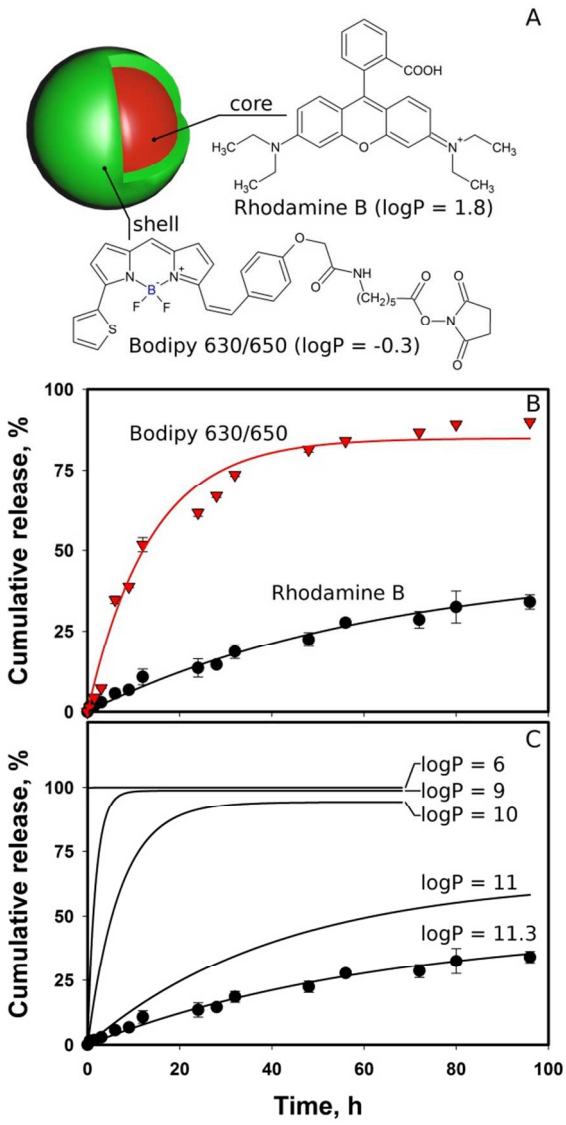

Figure 3. Validation of the method on the release of two compounds with different hydrophobicity based on published experimental results in [24]. (A) Schematics of the nanoparticle, where more hydrophobic compound is released from the core, and more hydrophilic – from the shell; logP values are shown for each compound. (B) Measured release of compounds (symbols) with computed releases using computational model with mass partitioning. (C) Calculated release curves from the core of the particle with different partitioning coefficients and comparison with the experiment).

Physical Chemistry Chemical Physics Accepted Manuscript

The interplay of partitioning and diffusion. We have used the findings in the experimental example shown in Figure 3 as a basis to analyze the impact of partitioning on the release rate of payload. The payload diffusivity D inside the nanoparticle was varied from 10^{-6} to 10^{-15} cm^2/s covering D characteristic to small molecules in liquids (~10^{-6} cm^2/s), in polymers (~10^{-8} cm^2/s), and its lower bound in solids (~10^{-13} cm^2/s) [26], while P was varied from 1 to 10^{12}. For P and D combinations, the cumulative mass release, *M*, curves were calculated and characterized by the exponent λ after fitting, according to the equation:

$$M = M_\infty \cdot [1 - \exp(-\lambda t)] \qquad (7)$$

where *t* is the time, and M_∞ is the maximum released mass; these curves are displayed in Figure 4.

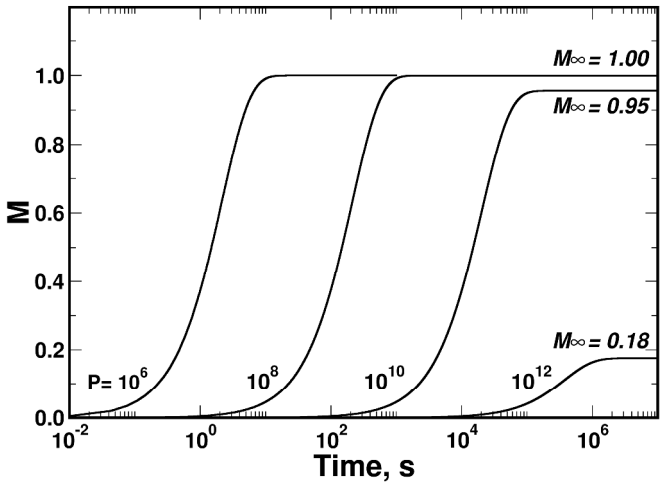

Physical Chemistry Chemical Physics Accepted Manuscript

Figure 4. Examples of cumulative mass release curves with D = 10^{-6} cm^2/s and particle concentration of $8.8 \cdot 10^3$ mL^{-1} , for different P. The curves are normalized by the total mass of the system. Here, M_∞ denotes the mass at the end of the release process, once the diffusion process stops.

Figure 5A shows λ as a function of P for different D values at $8.8 \cdot 10^3$ mL^{-1} concentration of nanoparticles, C, and reveals that for large D (fast payload diffusion inside nanoparticle) the increasing P monotonically lowers λ, *i.e.* slows down the release. Decreasing diffusivity of payload inside nanoparticle, the sensitivity of mass release to P gets reduced, unless P becomes larger than a certain value, *e.g.* λ(D=10^{-9} cm^2/s) is insensitive to P < 10^3, while for λ(D=10^{-14} cm^2/s) is insensitive to P < 10^8. Figure 5A illustrates that large P may dominate the release of payload and mask diffusion properties inside. Then, the only governing factor becomes the balance of concentrations across phase interface.

Because of the role of the P, the mass release from nanoparticles depends on concentration of nanoparticles: increasing the concentration of nanoparticles would reduce relative volume of the sink (buffer) and would affect the balanced concentrations. In our case we have varied surrounding sink volume for a single nanoparticle with radius from 300 to 1 nm and found the nanoparticle concentrations in the range of C = $8.8 \cdot 10^3$ – $2.4 \cdot 10^{11}$ mL^{-1}. Figure 5B shows λ dependence on P for D = 10^{-6}, 10^{-9} and 10^{-12} cm^2/s. The λ is characterized by two zones in the logarithmic scale where λ is constant at different P. This means that by increasing P, mass release kinetics does not change until it passes the transient zone of P values and gets constant

Physical Chemistry Chemical Physics Accepted Manuscript

again at larger P. Interestingly, λ can even increase (release gets faster) by increasing P, *e.g.* for $D = 10^{-12}$ cm^2/s (Figure 5B). This phenomenon can be explained by a very small sink value, leading to fast equilibration time between payload concentrations in nanoparticle and sink when P are large enough, and very limited release of mass from nanoparticle (see *Supplementary Material*, Figure S2). All together, we have a mass release process, which is controlled by mass partitioning at phase interface and the concentration of nanoparticles.

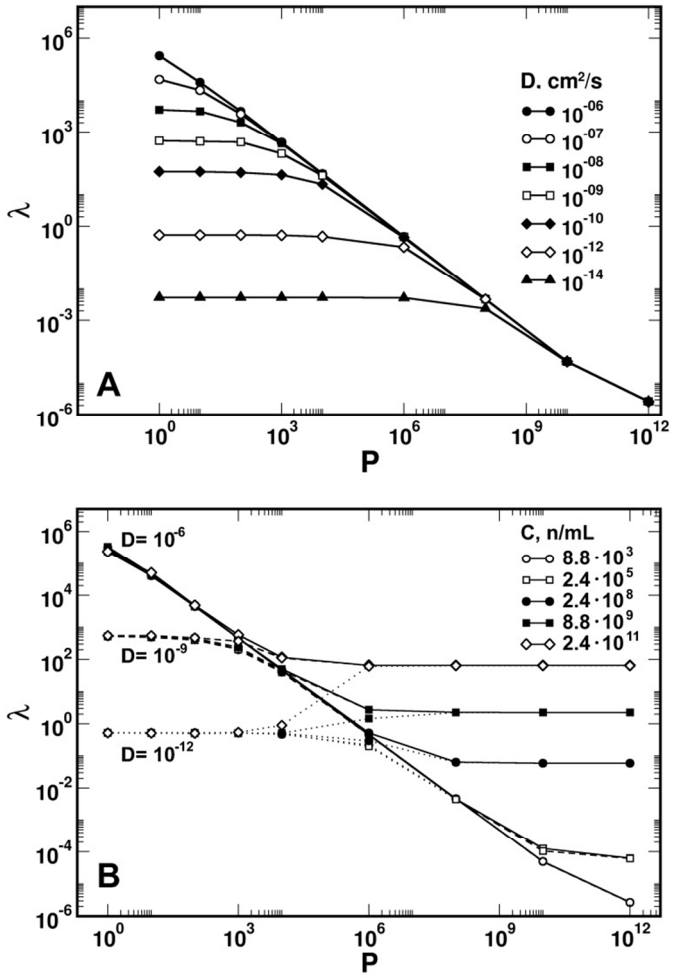

Physical Chemistry Chemical Physics Accepted Manuscript

Figure 5. Dependence of λ on P. (A) Increasing P reduces release kinetics (λ), which is especially pronounced for systems having fast-diffusing payload inside nanoparticle (larger D); while for very small D partitioning shows effects only at extreme values of P. (B) Larger concentrations of nanoparticle lead to less sink volume for payload release and affect λ through P. The increase in λ for small D is associated with very limited and therefore fast mass release from nanoparticles.

The frequent approach to model mass exchange has been by manipulating transport coefficients without more comprehensive analysis of other effects in the actual physical processes. We have presented the approach where we included mass partitioning and have shown that the mass balance at phase interface, which is governed by compound affinity to water or oil-like phases, modulates the mass transport. The validation example provides a strong proof that mass partitioning may not be only an important factor in mass exchange, but also it can be crucial in controlling the mass exchange and exchange kinetics. The presented approach is a relative simple numerical implementation to model partitioning, which could be further explored in a more sophisticated fashion, with elaboration of partitioning thermodynamics. This simplicity makes the implementation robust and easy to use in other transport modeling methods for studying physical aspects of transport. Partitioning of mass may have important implications in many areas of industries associated with mass exchange, as well as in biomedical and bioengineering fields focused on distribution and transport of therapeutic molecules.

Physical Chemistry Chemical Physics Accepted Manuscript

Acknowledgments

The authors acknowledge the Texas Advanced Computing Center (TACC) at The University of Texas at Austin for providing HPC resources that contributed to the results reported in this paper. This project was supported by the Houston Methodist Research Institute, grant OI 174028 of the Serbian Ministry of Education and Science (M.K); partial support from: the National Institute of Health (U54CA143837 – M.F., K.Y., U54CA151668 - M.F.), the Ernest Cockrell Jr. Distinguished Endowed Chair (M.F.), and the US Department of Defense (W81XWH-09-1-0212) (M.F.). Other authors declare no conflicts of interest.

References

[1] A. Ziemys, A. Grattoni, D. Fine, F. Hussain, and M. Ferrari, The Journal of Physical Chemistry B, 2010, **114**, 11117–11126

[2] A. Leo, C. Hansch, and D. Elkins, Chem. Rev., 1971, **71**, 525-616

[3] S. Simovic, and C. A. Prestidge, Eur. J. Pharm. Biopharm., 2007, **67**, 39-47

[4] H. Bunjes, The Journal of pharmacy and pharmacology, 2010, **62**, 1637-1645

[5] J. L. Arias, F. Linares-Molinero, V. Gallardo, and Á. V. Delgado, Eur. J. Pharm. Sci., 2008, **33**, 252-261

[6] M. L. Forrest, C. Y. Won, A. W. Malick, and G. S. Kwon, J. Control. Release, 2006, **110**, 370-377

[7] M. Thomas, I. Slipper, A. Walunj, A. Jain, M. Favretto, P. Kallinteri, and D. Douroumis, Int. J. Pharm., 2010, **387**, 272-277

Physical Chemistry Chemical Physics Accepted Manuscript

[8] L. B. Jensen, E. Magnussson, L. Gunnarsson, C. Vermehren, H. M. Nielsen, and K. Petersson, Int. J. Pharm., 2010, **390**, 53-60

[9] R. Mannhold, G. I. Poda, C. Ostermann, and I. V. Tetko, J. Pharm. Sci., 2009, **98**, 861-893

[10] J. Siepmann, and F. Siepmann, J. Control. Release, 2012, **161**, 351-362

[11] J. D. Martin, and S. D. Hudson, New Journal of Physics, 2009, **11**, 115005

[12] J. Kushner, W. Deen, D. Blankschtein, and R. Langer, J. Pharm. Sci., 2007, **96**, 3236-3251

[13] A. M. Barbero, and H. Frasch, Ann. Biomed. Eng., 2005, **33**, 1281-1292

[14] J. E. Rim, P. M. Pinsky, and W. W. van Osdol, Ann. Biomed. Eng., 2005, **33**, 1422-1438

[15] C.-W. Hwang, D. Wu, and E. R. Edelman, Circulation, 2001, **104**, 600-605

[16] M. Kojic, N. Filipovic, S. Vulovic, and S. Mijailovic, Communications in Numerical Methods in Engineering, 1998, **14**, 381-392

[17] M. Kojic, R. Slavkovic, M. Zivkovic, and N. Grujovic, (University of Kragujevac; R&D Center for Bioengineering, Kragujevac, 1998).

[18] A. Ziemys, M. Kojic, M. Milosevic, and M. Ferrari, Phys. Rev. Lett., 2012, **108**, 5

[19] A. Ziemys, M. Kojic, M. Milosevic, N. Kojic, F. Hussain, M. Ferrari, and A. Grattoni, J. Comput. Phys., 2011, **230**, 5722–5731

[20] J. C. Phillips, R. Braun, W. Wang, J. Gumbart, E. Tajkhorshid, E. Villa, C. Chipot, R. D. Skeel, L. Kalé, and K. Schulten, J. Comput. Chem., 2005, **26**, 1781-1802

[21] W. L. Jorgensen, J. Chandrasekhar, J. D. Madura, R. W. Impey, and M. L. Klein, J. Chem. Phys., 1983, **79**, 926-935

[22] K. Vanommeslaeghe, E. Hatcher, C. Acharya, S. Kundu, S. Zhong, J. Shim, E. Darian, O. Guvench, P. Lopes, and I. Vorobyov, J. Comput. Chem., 2010, **31**, 671-690

[23] M. Kojic, N. Filipovic, B. Stojanovic, and N. Kojic, *Computer modeling in bioengineering: Theoretical background, examples and software* (J Wiley and Sons, 2008), Vol. 195.

Physical Chemistry Chemical Physics Accepted Manuscript

[24] G. U. Ruiz-Esparza, S. Wu, V. Segura-Ibarra, F. E. Cara, K. W. Evans, M. Milosevic, A. Ziemys, M. Kojic, F. Meric-Bernstam, and M. Ferrari, Adv. Funct. Mater., 2014,

[25] P. Norvaisas, and A. Ziemys, J. Pharm. Sci., 2014,

[26] E. Cussler, *Diffusion: Mass transfer in fluid systems* (Cambridge Univ Pr, 1997).

[27] C. Washington, Int. J. Pharm., 1989, **56**, 71-74

Physical Chemistry Chemical Physics Accepted Manuscript

Figure legends

Figure 1. Schematics of studied systems. The structure and dimensions of MD model to simulate partitioning P between octanol and water phases (**A**). The implementation of partitioning in the FE model, where increments of concentrations at the common node (J^S and J^f) are related as $\Delta C_f = p\Delta C_s$, equation (6) (**B**).

Figure 2. Interplay of diffusivity and partitioning in mass distribution. The redistribution of a hydrophobic molecule (p-ethylphenol) across octanol/water system; the representative snapshots of the initial (**A**) and final (**B**) configurations after 20 ns from MD simulations. The calculated density and diffusivity distributions of *p*-ethylphenol across octanol/water phases (**C**). The calculated concentration redistribution by FE in a system having 1M concentration on the left-half and no partition (**D**) and having logP = 1 (**E**).

Figure 3. Mass redistribution in the fluidic system separated by imaginary phase separation at zero. While diffusivities are equal on left and right of the reservoir, those halves are separated different logP: logP = 1 (no partitioning, **A**), logP = 1 (**B**), and logP = 2 (**C**).

Figure 3. Validation of the method on the release of two compounds with different hydrophobicity based on published results in [22]. The schematics of the nanoparticles, where more hydrophobic compound is released from the core and more hydrophilic – from the shell; logP values provided for each compound (**A**). The measure release of compounds (symbols) with best fit using computational model incorporating mass partitioning (**B**). The calculated release curves from the core of the particle with different partitioning coefficients for comparison to the experiment (**C**).

Physical Chemistry Chemical Physics Accepted Manuscript

Figure 1

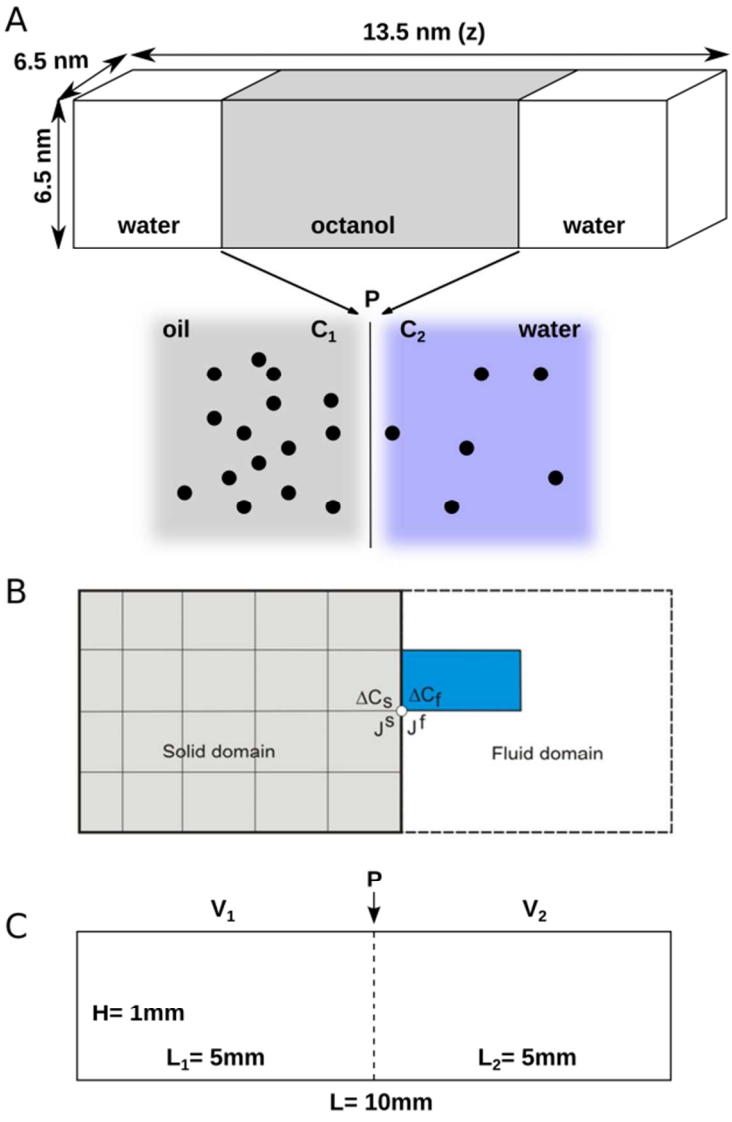

Physical Chemistry Chemical Physics Accepted Manuscript

Figure 2

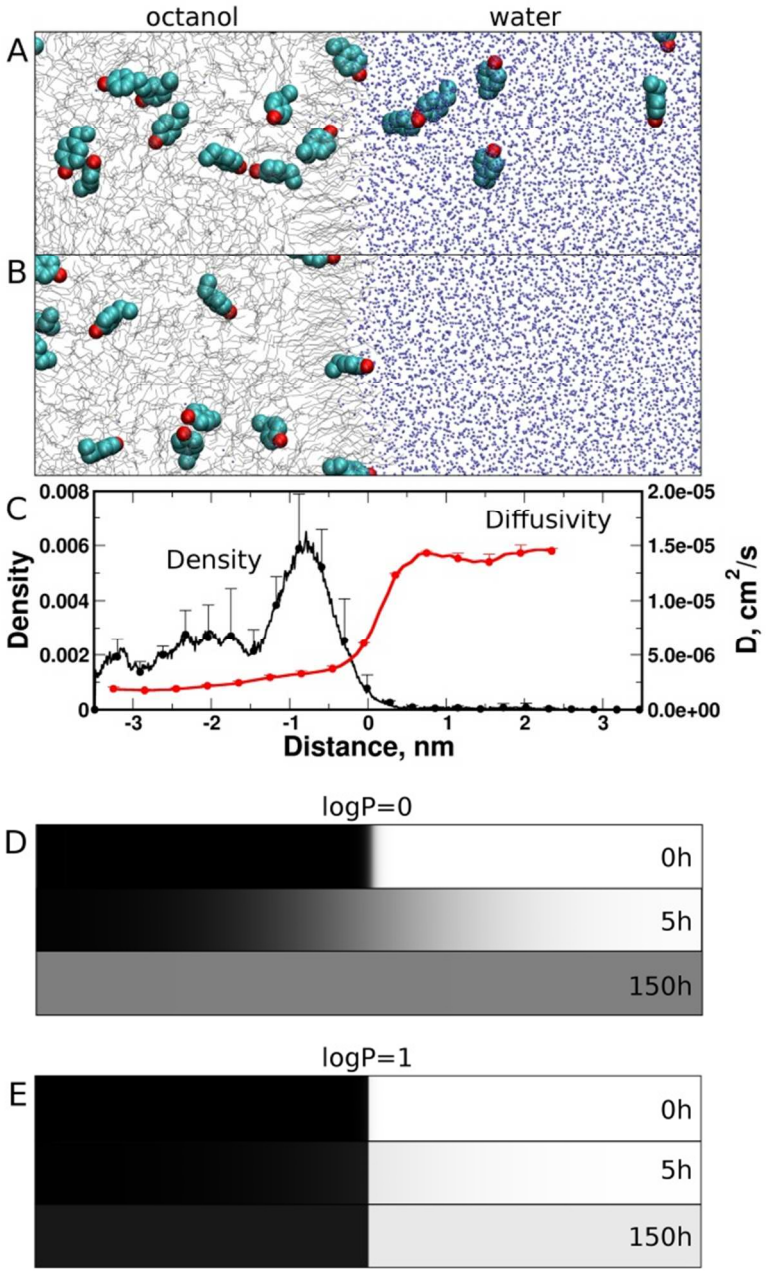

Physical Chemistry Chemical Physics Accepted Manuscript

Figure 3

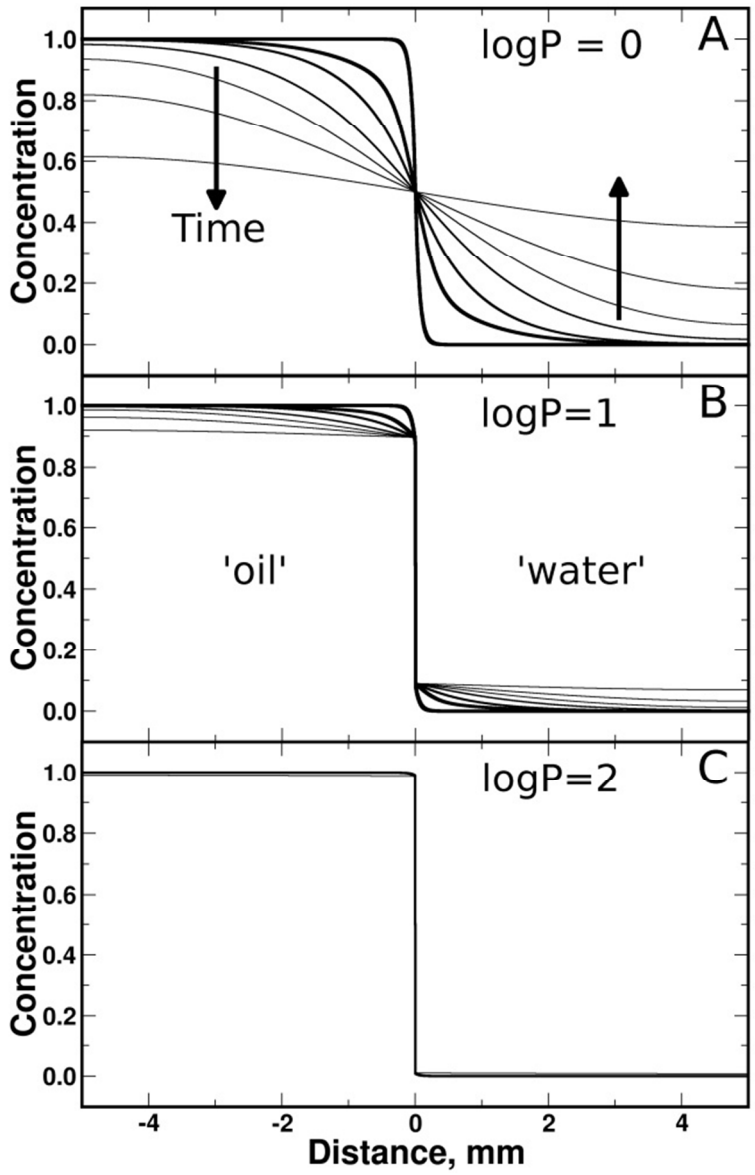

Physical Chemistry Chemical Physics Accepted Manuscript

Figure 4

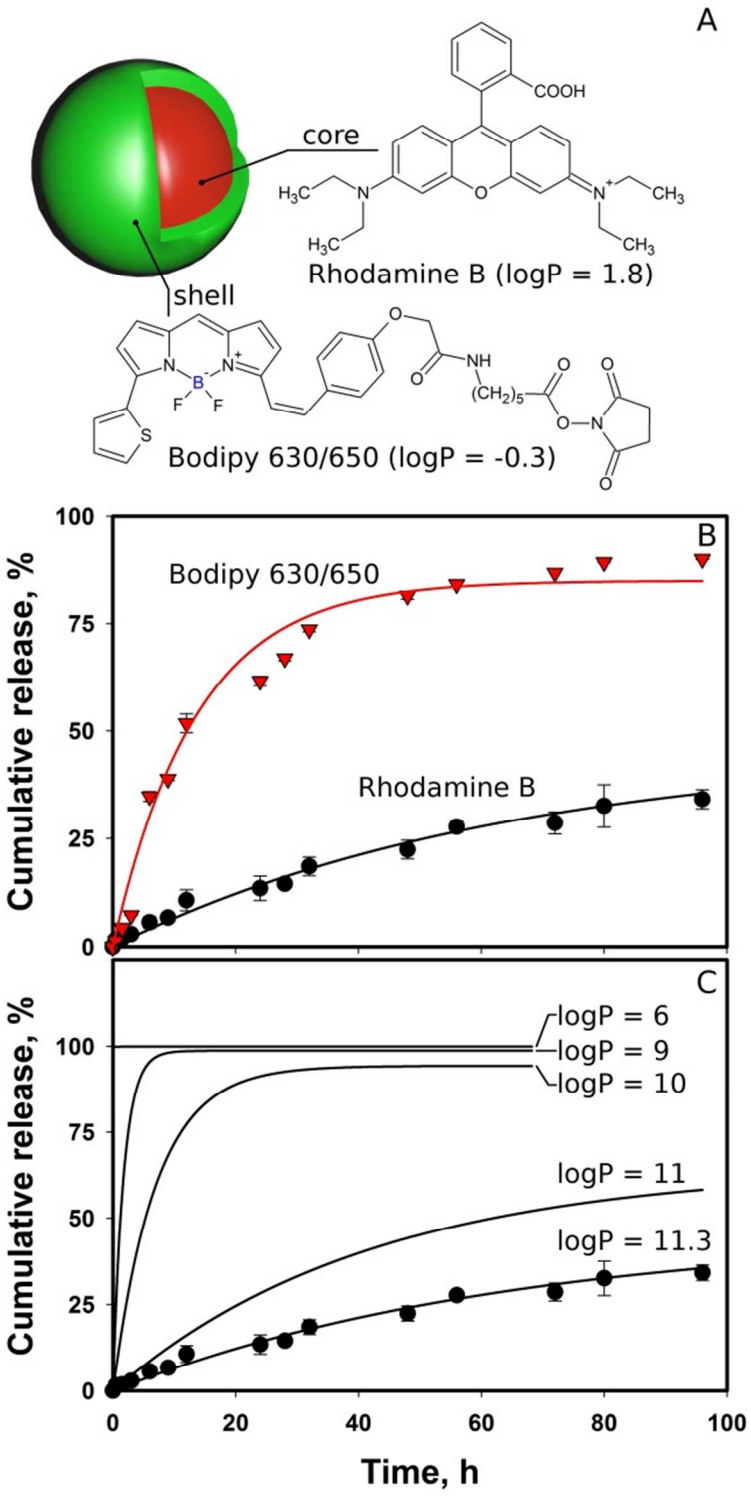

Physical Chemistry Chemical Physics Accepted Manuscript